Contents lists available at ScienceDirect

Comptes Rendus Chimie

www.sciencedirect.com

CrossMark

Full paper/Mémoire

Preparation, characterization and application of RHA/TiO$_2$ nanocomposites in the acetylation of alcohols, phenols and amines

Mohadeseh Seddighi, Farhad Shirini[*], Omid Goli-Jolodar

Department of Chemistry, College of Science, University of Guilan, Rasht, 41335, I.R. Iran

A B S T R A C T

In this work, anatase-phase nano-titania was prepared by embedding in rice husk ash, and identified using a variety of techniques. The obtained nanocomposite (RHA/TiO$_2$) was used as a green and inexpensive catalyst for the promotion of the acetylation of alcohols, phenols and amines with Ac$_2$O at room temperature under solvent free conditions. The procedure gave the products in excellent yields during all reaction times. Also this catalyst can be reused for several times without loss of its catalytic activity.

© 2016 Académie des sciences. Published by Elsevier Masson SAS. All rights reserved.

1. Introduction

Protection of functional groups is often necessary during a multistep organic synthesis, so the development of economical and efficient methods for this purpose is very important. Hydroxyl and amino groups in alcohols, phenols and amines are often present in organic molecules, and their protection is an important process during organic reactions. Among various procedures for the protection of hydroxyl and amino groups, acetylation with acetic anhydride or acetyl chloride in the presence of an acidic or basic catalyst is an efficient and common route due to the stability of the products in acidic media and easy introduction and removal of the acetyl group. For this purpose many Brönsted and *Le*wis acidic catalysts have been used [1–6]. Although these methods are improved, most of them suffer from disadvantages such as long reaction times, use of organic solvents, expensive catalysts, use of excess amounts of the acylating agents and harsh reaction conditions. Therefore there is still a need to find an alternative method which might be mild and catalytically and economically efficient.

In recent years, synthesis of nanocrystalline metal oxides has attracted much attention due to their unusual catalytic properties compared to bulk metals [7]. Among various metal oxides, TiO$_2$ nanoparticles is one of the most utilized ones which have been widely investigated as the catalyst, pigment, food coloring substance, etc [8–9]. Preparation of the non-agglomerated TiO$_2$ nanoparticles, with a narrow size distribution in anatase form, is very important to achieve higher catalytic activity and more readily handling than the commercial TiO$_2$ [10–11]. On the basis of this subject, the synthesis of TiO$_2$ over a silica support was explored as a useful way for preventing the agglomeration and formation of dispersed TiO$_2$ aggregates [12]. Siliceous materials are desirable because they are chemically inert and have a high specific surface area and thermal stability.

Rice husk, the outer covering of rice grains, is one of the main agricultural residues which is obtained during the

* Corresponding author.
E-mail address: shirini@guilan.ac.ir (F. Shirini).

milling process. Application of rice husk as an energy source for biomass power plants, rice mills and brick factories is increasing due to its high calorific power [13]. In this combustion, rice husk ash (RHA) is produced. RHA contains a considerable amount of amorphous silica up to 80% and small proportion of impurities such as K_2O, Na_2O and Fe_2O_3 [14].

In recent years, investigation on the application of TiO_2-based reagents in organic reactions became an important part of our ongoing research program [15–17]. In continuation of these studies and because that RHA possesses high silica content, we were interested to investigate the possibility of the preparation of anatase-phase TiO_2 over this reagent.

2. Experimental

2.1. General

Chemicals were purchased from Fluka, Merck, and Aldrich chemical companies. All yields refer to the isolated products. Products were characterized by comparison of their physical constants, IR and NMR spectroscopy with authentic samples and those reported in the literature. The purity determination of the substrate and reaction monitoring were accompanied by TLC on silicagel polygram SILG/UV 254 plates.

2.2. Instrumentation

The FT-IR spectra were run on a VERTEX 70 Brucker company (Germany). Scanning election microphotographs were obtained on a SEM-Philips XL30. X-ray diffraction (XRD) measurements were performed at room temperature on a Siemens D-500 X-ray diffractometer (Germany), using Ni-filtered Co Kα radiation ($\lambda = 0.15418$ nm).

2.3. Preparation of RHA/TiO_2 nanocomposites

1.0 g of rice husk ash (used in our previous report [18])in absolute ethanol (6 mL) was stirred for 30 min at room temperature. Then the required amount of titanium tetraisopropoxide (TTIP) (volume ratio TTIP:EtOH of 1:6) was added dropwise to the solution with stirring for 2 h. In continue, deionized water was slowly added to the resulting mixture (TTIP:water with a ratio of 1:60) and the stirring was maintained for 2 h to hydrolyze the remaining TTIP completely. The prepared material was separated by filtration, washed with water, and dried at 80 °C in an oven. Finally, the obtained solid was calcinated at 500 °C for 3 h to obtain RHA/TiO_2 nonocomposites. [Caution: Throughout the subsequent discussion, the samples will be named by indicating the titania content and support, as RHA/TiO_2(20%), RHA/TiO_2(30%) and RHA/TiO_2(50%).]

2.4. General procedure for acetylation with Ac_2O catalyzed by RHA/TiO_2(30%)

1 mmol of the substrate (alcohol, phenol or amine) was added to a mixture of RHA/TiO_2(30%) (20 mg) and acetic anhydride (1.5 mmol per OH/NH_2 group) and the resulting

mixture was stirred at room temperature. After completion of the reaction (mentioned by TLC), dichloromethane (20 mL) was added and the catalyst was separated by filtration. The organic phase was washed with 10% aqueous solution of sodium bicarbonate (2 × 20 mL) and dried over Na_2SO_4. The solvent was removed under reduced pressure to afford the desired product in good to high yields. The spectral (IR, ^1H and ^{13}C NMR) data of new compounds are presented below:

Benzene-1,2,3-triyl triacetate: White solid; IR (neat) $\nu = 1765$ cm^{-1}; ^1H NMR (CDCl$_3$, 400 MHz): $\delta = 2.31$ (s, 6H, CH$_3$), 2.32 (s, 3H, CH$_3$),7.14 (d, $J = 8.2$ Hz, 2H, ArH), 7.29 (dd, $J = 8.3$ and 0.8 Hz, 1H, ArH) ppm; ^{13}C NMR (CDCl$_3$, 100 MHz): $\delta = 20.6$, 21.0, 121.1, 126.4, 135.1, 143.9, 167.4, 168.3 ppm.

N-(naphthalen-1-yl)acetamide: White solid; IR (neat) ν: 3295, 1635 cm^{-1}; ^1H NMR (CDCl$_3$, 400 MHz): $\delta = 2.30$ (s, 3H, CH$_3$), 7.45–7.87 (m, 8H, ArH, NH) ppm; ^{13}C NMR (CDCl$_3$, 100 MHz): $\delta = 22.8$, 118.5, 122.3, 122.8, 125.2, 126.1, 127.3, 127.8, 128.4, 128.5, 133.1, 169.9 ppm.

2.5. Catalyst characterization

2.5.1. FT-IR analysis

Fig. 1 shows the FT-IR spectra of nano-TiO_2 (anatase), RHA and 20, 30 and 50 W% RHA/TiO_2. In all cases, the peaks at 3400 and 1630 cm^{-1} are attributed to the stretching and bending modes of the hydroxyl groups of Si–OH or Ti–OH and the adsorbed water [19]. The strong peak at 1100 cm^{-1} and the peaks at 801 and 468 cm^{-1} are assigned to the asymmetric stretching, symmetric stretching and bending modes of Si–O–Si, respectively. Because the vibration modes of Ti–O–Ti lie in the range of 500–700 cm^{-1} (Fig. 1, spectrum of TiO_2) [20], the peaks appearing at 500–700 cm^{-1} in the prepared samples can be attributed to Ti–O–Ti (Fig. 1, spectra of RHA/TiO_2 nanocomposites). Increasing the intensity of these bands by increasing the titanium content of the samples can be described on the basis of this fact. Theoretically, the stretching vibration of Ti–O–Si appeared as a weak peak at 960 cm^{-1}, whereas such a peak was not observed in the prepared samples. So, it could be resulted from the FT-IR spectra and there is no binding between TiO_2 and SiO_2, and titania is only embedded into the RHA matrix [10].

2.5.2. Powder X-ray diffraction

Fig. 2 represents the X-ray diffraction (XRD) patterns of the RHA and RHA/TiO_2 nanocomposites. The broad peak appeared around 2θ equal to 22 in the RHA pattern clearly indicating that the silica of rice husk ash is mainly in the amorphous form [21]. The peaks appearing around 2$\theta = 25.3$, 37.8, 47.8, 54.1 and 62.3 in RHA/TiO_2 nanocomposites are related to the (101), (004), (200), (105) and (211) reflections which indicate that the anatase phase is the only phase present in all the prepared materials [22–23]. The intensity of anatase peaks increased by increasing in the titania contents, however broadening of these peaks show that the nanocomposite particles have very small size. These observations strongly suggested that not only the RHA inhibited the formation of the rutile
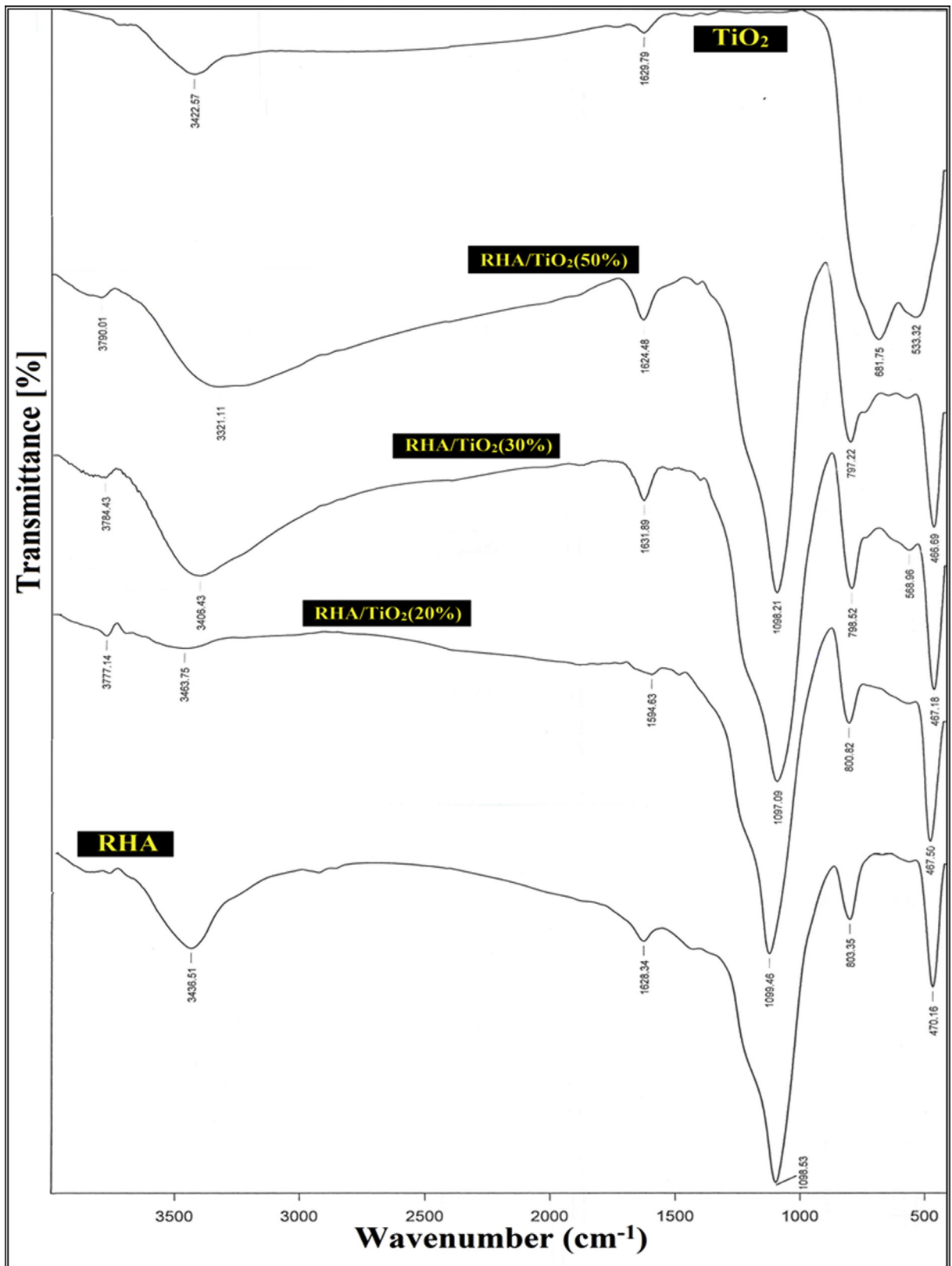
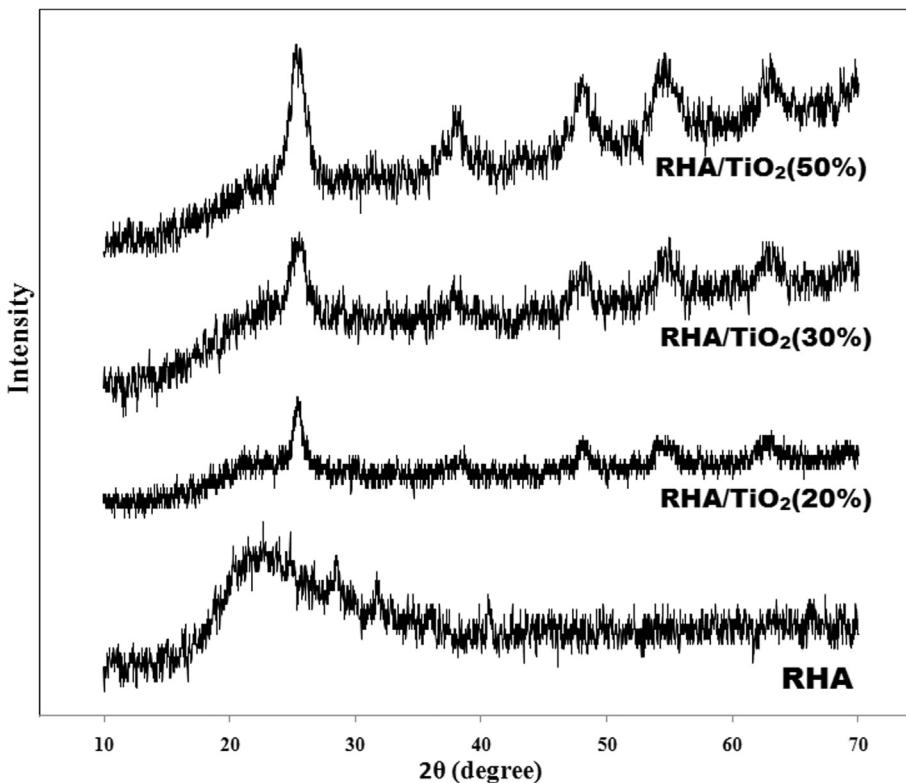**Fig. 1.** FT-IR spectra of RHA, TiO₂ and various RHA/TiO₂ nanocomposites.

Fig. 2. XRD patterns of RHA and various samples of RHA/TiO$_2$ nanocomposites.

Table 1
XRD data of RHA/TiO$_2$ nanocomposites.

Entry	Nanocomposite	2θ	Peak width [FWHM]	Size [nm]
1	RHA/TiO$_2$(20%)	25.35	0.40	20
2	RHA/TiO$_2$(30%)	22.38	0.38	21
3	RHA/TiO$_2$(50%)	25.36	0.36	22

phase, but also inhibited growth of crystal grain of titan [24].

The average crystalline sizes of nanocomposites were estimated by XRD using Scherrer's equation by considering the full width and half maximum (FWHM) value (Table 1). As can be seen, all of the synthesized nanocomposites have almost the same crystalline sizes.

2.5.3. SEM and TEM analysis

Scanning electron microscopy (SEM) and transmission electron microscopy (TEM) were performed for the
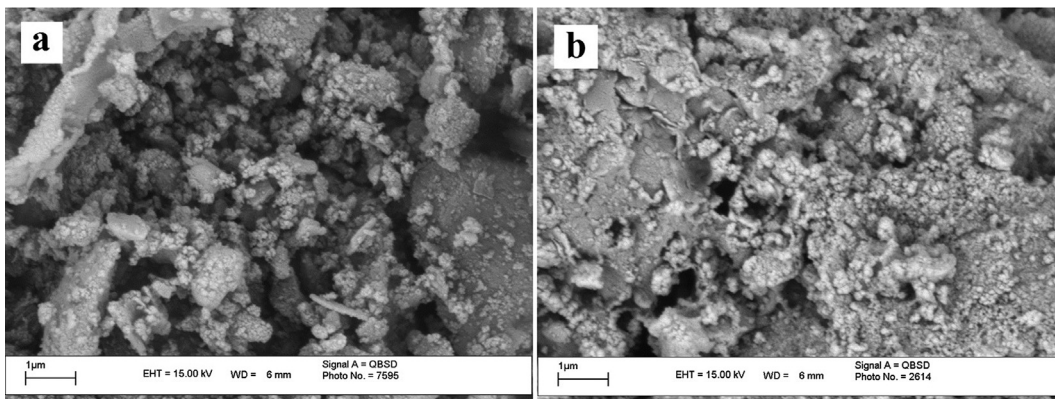
Fig. 3. SEM images of RHA (a) and RHA/TiO$_2$(30%) (b).
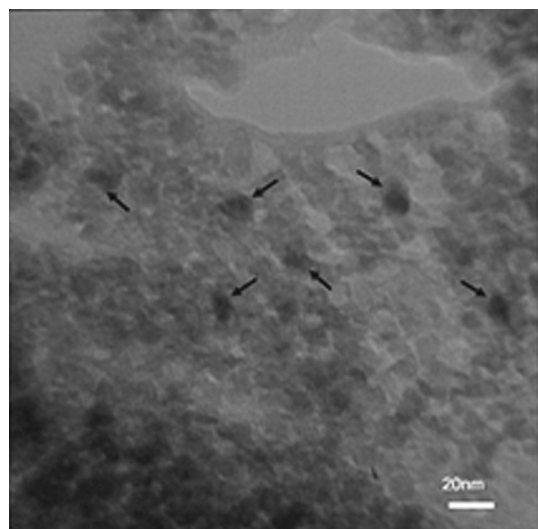
Fig. 4. TEM images of RHA/TiO$_2$ (30%).

determination of the size distribution, particle shape and surface morphology, as shown in Fig. 3 and Fig. 4. It should be noted that these analysis were carried out on RHA/TiO$_2$(30%) (the best ratio of RHA/TiO$_2$ with the highest catalytic activity was determined in the acetylation of 4-chlorobenzyl alcohol). The SEM pictures show that RHA has a porous and irregular shape [25], and the porosity was substantially maintained over dispersion of TiO$_2$ in RHA/TiO$_2$(30%). It is clear from the TEM images that TiO$_2$ nanoparticles, which can be seen as dark particles, are spherical with average size less than 10 nm in diameter, which have been dispersed in the matrix of RHA, as shown in Fig. 4.
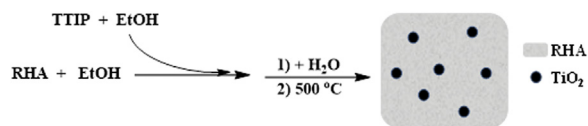
Scheme 1. Preparation of RHA/TiO$_2$ nanocomposites.

Table 2
Optimization of the best ratio of RHA/TiO$_2$ nanocomposites in the acetylation of 4-chlorobenzyl alcohol.

Entry	Catalyst	Time (min)	Conversion (%)
1	RHA/TiO$_2$(20%)	15	85
2	RHA/TiO$_2$(30%)	8	100
3	RHA/TiO$_2$(50%)	8	100

2.5.4. N$_2$ adsorption−desorption measurements

N$_2$ adsorption−desorption measurements based on BET and BJH methods, which have been a powerful tool for nano- or meso-porous material characterization, were performed to obtain more information about the catalyst. The adsorption−desorption isotherm of RHA and RHA/TiO$_2$(30%) nanocomposites is shown in Fig. 5a. Both samples exhibited a type IV isotherm with H$_3$ hysteresis loop categories according to the literature, which indicates that
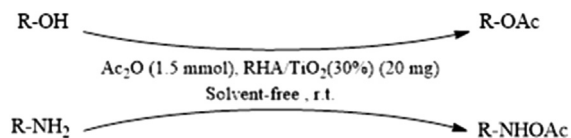
Scheme 2. Acetylation of alcohols, phenols and amines catalyzed by RHA/TiO$_2$(30%).
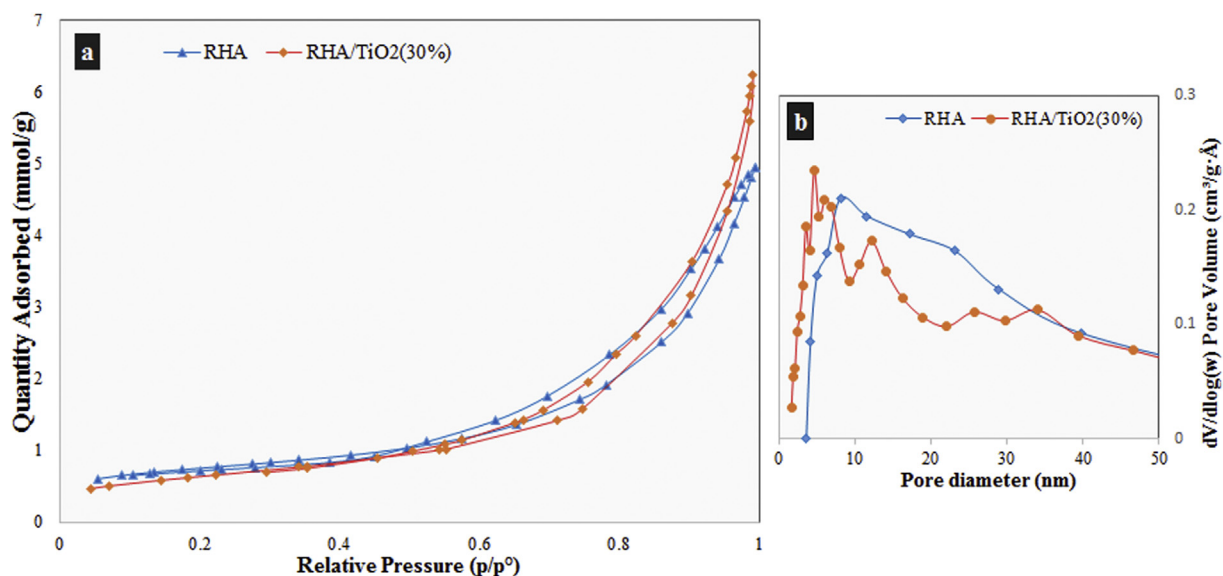
Fig. 5. The N$_2$ adsorption−desorption isotherm (a), and pore size distribution (b) of RHA and RHA/TiO$_2$(30%).

Table 3
Acetylation of alcohols, phenols and amines in the presence of RHA/TiO$_2$(30%) under solvent-free conditions.
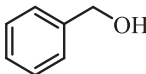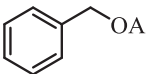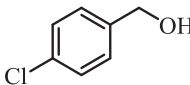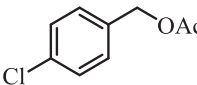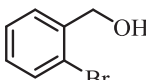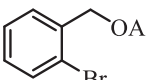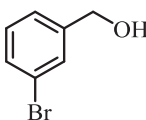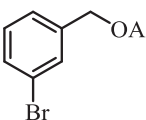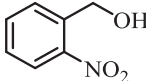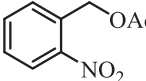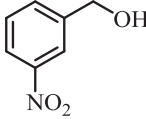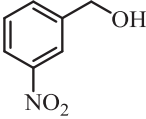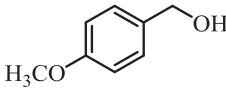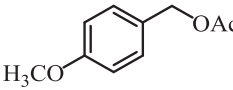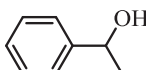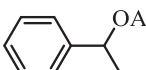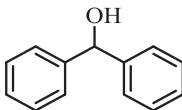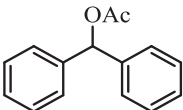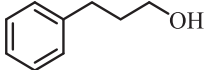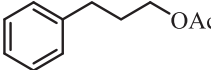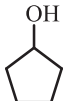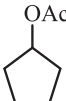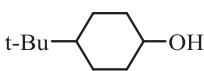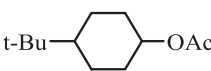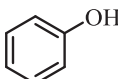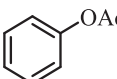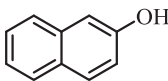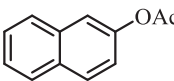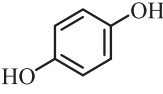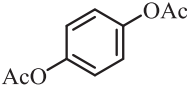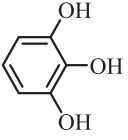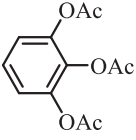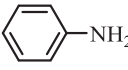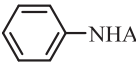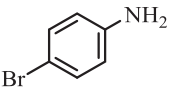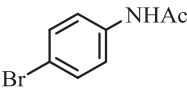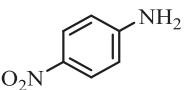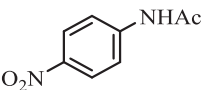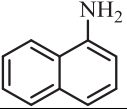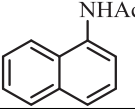
Entry	Aldehyde	Product	Time (min)	Yield (%)[a]
1			7	96
2			8 (8,9,10,10)[b]	97 (95,96,97,94)
3			10	91
4			10	93
5			10	94
6			20	94
7			10	95
8			15	90
9			12	88
10			14	93
11			0.5	96
12			0.5	96
13			12	94
14			15	90

Table 3 (*continued*)

Entry	Aldehyde	Product	Time (min)	Yield (%)[a]
15	HO–C6H4–OH (1,4)	AcO–C6H4–OAc (1,4)	20	91
16[c]	1,2,3-trihydroxybenzene (OH, OH, OH)	1,2,3-triacetoxybenzene (OAc, OAc, OAc)	25	90
17	C6H5–NH2	C6H5–NHAc	7	93
18	Br–C6H4–NH2	Br–C6H4–NHAc	7	93
19	O2N–C6H4–NH2	O2N–C6H4–NHAc	10	92
20	naphthyl–NH2	naphthyl–NHAc	7	94

[a] Isolated yields.
[b] Results obtained using the recovered catalyst.
[c] 40 mg of the catalyst was used.

the samples are mesoporous materials with slit-like pores [26]. These results also prove that the textural properties of RHA were substantially maintained over the preparation of the nanocomposite. The specific BET surface areas of RHA and RHA/TiO$_2$(30%) are 57 and 50 m^2/g, respectively. Furthermore, the curves of pore size distribution evaluated from desorption data by utilizing the BJH model are also shown in Fig. 5b. These curves show that there are some particles with average size less than 10 nm in diameter in RHA/(30%) which do not exist in RHA. These particles can be attributed to the TiO$_2$ nanoparticles.

3. Results and discussion

On the basis of the information obtained from the studies on RHA/TiO$_2$ nanocomposites, it is expected that this reagent can be used as a catalyst for the promotion of the organic reactions. So this reagent was used in the promotion of the conversion of alcohols, phenols and amines to their corresponding acetates and/or amides with acetic anhydride (Scheme 1).

In the first step we focused our attention toward the optimization of the ratio of RHA to TiO$_2$ for obtaining the highest catalytic activity. For this purpose, acetylation of 4-chlorobenzyl alcohol was studied and the best results were obtained using RHA/TiO$_2$(30%) (Table 2). Further increase in this ratio did not improve the activity of the prepared nanocomposite. Then for obtaining the optimum reaction conditions, we studied the influence of the following factors on the acetylation of 4-chlorobenzyl alcohol with

acetic anhydride: i) the amounts of the catalyst; ii) solvent or solvent-less media and iii) temperature. The obtained results clarified that the best conditions are the ones which are shown in Scheme 2.

After optimization of the reaction conditions, different types of alcohols were subjected to the acetylation using this method (Table 3). Acetylation of various benzylic alcohols containing electron-withdrawing and electron-donating substituents proceeded efficiently with high isolated yields (Table 3, Entries 1–7). Primary, secondary and
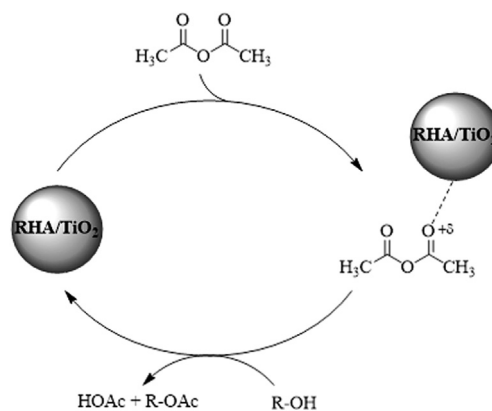
Scheme 3. Proposed mechanism of the reaction.

Table 4

Comparison of the results of the acetylation of benzyl alcohol catalyzed by RHA/TiO$_2$(30%) with those obtained by using some of the reported catalysts.

Entry	Catalyst (loading)	Reaction conditions	Time (min)	Yield (%)	[Ref.]
1	Zeolite HSZ-360 (20 mg)	60 °C/Neat	60	84	[1]
2	Cu(OTf)$_2$ (2.5 mol%)	r.t./CH$_2$Cl$_2$	30	97	[2]
3	RuCl$_3$ (5 mol%)	r.t./CH$_3$CN	10	98	[3]
4	Saccharinsulfonic acid (5 mol%)	Reflux/CH$_2$Cl$_2$	120	85	[4]
5	RiH (300 mg)	80 °C/Neat	60	94	[5]
6	RHA (50 mg)	80 °C/Neat	15	93	[6]
7	TiO$_2$ (30 mg)	100 °C/Neat	15	95	This work
8	RHA/TiO$_2$(30%) (20 mg)	r.t./Neat	0.5	95	This work

tertiary aliphatic alcohols were also efficiently converted to their corresponding acetates in almost quantitative yields at room temperature (Table 3, Entries 8–12). No elimination and rearrangement by-products were observed at all. Phenol and its derivatives also undergo acetylation easily using this method and their corresponding acetates can be isolated in excellent yields (Table 3, Entries 13–16). In the case of pyrogallol, higher amounts of the catalyst are needed due to high steric hindrance (Table 3, Entry 16). This method is also very useful for the acetylation of amines with acetic anhydride. All reactions are performed under mild reaction conditions in very short reaction times with high yields (Table 3, Entries 17–20).

To check the reusability of the catalyst, the reaction of 4-chlorobenzyl alcohol and acetic anhydride under the optimized reaction conditions was studied. When the reaction was completed, dichloromethane was added and the catalyst was separated by filtration. The recovered catalyst was washed with dichloromethane, dried and reused for the same reaction. This process was carried out over five runs and all reactions led to the desired products with high efficiency (Table 3, Entry 2).

The possible mechanism for the acetylation of alcohols, phenols and amines in the presence of RHA/TiO$_2$(30%) as a promoter is shown in Scheme 3. On the basis of this mechanism, RHA/TiO$_2$(30%) catalyzes the reaction by the electrophilic activation of Ac$_2$O to form a zwitterionic species, making the carbonyl group susceptible to nucleophilic attack by the substrate. Successive elimination of CH$_3$CO$_2$H results in the formation of the requested product and regenerates RHA-SO$_3$H in the reaction mixture.

To illustrate the efficiency of the proposed method, Table 4 compares our results in the acetylation of 4-chlorobenzyl alcohol with those reported by using the relevant reagents in the literature. It is clear that the present method is superior in terms of the reaction time and catalyst amount, especially compared with rice husk (RiH), rice husk ash (RHA) and TiO$_2$ (Table 4, Entries 5–7).

4. Conclusions

In conclusion, rice husk ash was used as a silica support for the synthesis of anatase-phase titania nanoparticles and a RHA/TiO$_2$ nanocomposite was obtained. Then, a simple and efficient protocol for the acetylation of alcohols, phenols and amines was developed using this nanocomposite. The methodology has several advantages such as: (i) high reaction rates and excellent yields, (ii) no side reactions, (iii) ease of preparation and handling of the catalyst, (iv) cost efficiency and effective reusability of the catalyst, (v) use of an inexpensive catalyst with lower loading and (vi) a simple experimental procedure and solvent free conditions. Further work to explore this catalyst in other organic transformations is in progress.

References

[1] R. Ballini, G. Bosica, S. Carloni, L. Ciaralli, R. Maggi, G. Sartori, Tetrahedron Lett. 39 (1998) 6049–6052.
[2] P. Saravanan, V.K. Singh, Tetrahedron Lett. 40 (1999) 2611–2614.
[3] S.K. De, Tetrahedron Lett. 45 (2004) 2919–2922.
[4] F. Shirini, M.A. Zolfigol, M. Abedini, Monatsh. Chem. 140 (2009) 1495–1498.
[5] F. Shirini, S. Akbari-Dadamahaleh, A. Mohammad-Khah, A. Aliakbar, C. R. Chim. 17 (2014) 164–170.
[6] F. Shirini, S. Akbari-Dadamahaleh, A. Mohammad-Khah, Phosphorus, Sulfur Silicon Relat. Elem. 189 (2014) 577–586.
[7] Z. Zhang, C.C. Wang, R. Zakaria, J.Y. Ying, J. Phys. Chem. B 102 (1998) 10871–10878.
[8] S.M. Gupta, M. Triptha, Chin. Sci. Bull. 56 (2011) 1639–1657.
[9] X. Chen, S.S. Mao, Chem. Rev. 107 (2007) 2891–2959.
[10] K.Y. Jung, S.B. Park, J. Photochem. Photobiol., A 127 (1999) 117–122.
[11] J. Aguado, R. Van-Grieken, M. Lopez-Munoz, J. Marugan, Appl. Catal. A: Gen. 312 (2006) 202–212.
[12] R. van Grieken, J. Aguado, M.J. Lopez-Munoz, J. Marugan, J. Photochem. Photobiol., A 148 (2002) 315–322.
[13] C. Real, M.D. Alcalá, J.M. Criado, J. Am. Ceram. Soc. 79 (1996) 2012–2016.
[14] Q. Feng, H. Yamamichi, M. Shoya, S. Sugita, Cem. Concr. Res. 34 (2004) 521–526.
[15] F. Shirini, M.A. Khoshdel, M. Abedini, S.V. Atghia, Chin. Chem. Lett. 22 (2011) 1211–1214.
[16] F. Shirini, S.V. Atghia, M.G. Jirdehi, Catal. Commun. 18 (2012) 5–10.
[17] F. Shirini, M. Abedini, S.A. Kiaroudi, Phosphorus Sulfur 189 (2014) 1279–1288.
[18] F. Shirini, M. Mamaghani, M. Seddighi, Catal. Commun. 36 (2013) 31–37.
[19] N.P. Hung, N.T.V. Hoan, N.V. Nghia, Nanosci. Nanotechnol. 3 (2013) 19–25.
[20] D.A. Kumar, J.M. Shyla, F.P. Xavier, Appl. Nanosci. 2 (2012) 429–436.
[21] H.T. Jang, Y. Park, Y.S. Ko, J.Y. Lee, B. Margandan, Int. J. Greenh. Gas Control 3 (2009) 545–549.
[22] S. Wang, K. Wang, J. Jehng, L. Liu, Front. Environ. Sci. Eng. 6 (2012) 304–312.
[23] I. Pavlovska, K. Malnieks, G. Mezinskis, L. Bidermanis, M. Karpe, Surf. Coat. Technol. 258 (2014) 206–210.
[24] J. Yang, J. Zhang, L. Zhu, S. Chen, Y. Zhang, Y. Tang, Y. Zhu, Y. Li, J. Hazard. Mater. B 137 (2006) 952–958.
[25] G.A. Habeeb, H.B. Mahmud, Mater. Res. 13 (2010) 185–190.
[26] J.B. Condon, Surface Area and Porosity Determinations by Physisorption, Elsevier, 2006. Chapter 1, pp. 1–27.